Marquette University

e-Publications@Marquette

Detection of Hydrogen Peroxide Production in the Isolated Rat Lung Using Amplex Red

Said H. Audi
Marquette University, said.audi@marquette.edu

Nina Friedly
Marquette University

Ranjan K. Dash
Medical College of Wisconsin

Andreas M. Beyer
Medical College of Wisconsin, Milwaukee

Anne V. Clough
Marquette University, anne.clough@marquette.edu

See next page for additional authors

Recommended Citation

Authors
Said H. Audi, Nina Friedly, Ranjan K. Dash, Andreas M. Beyer, Anne V. Clough, and Elizabeth R. Jacobs

Detection of Hydrogen Peroxide Production in the Isolated Rat Lung Using Amplex Red

Said H. Audi
Medical College of Wisconsin Department of Biomedical Engineering, Marquette University, Milwaukee, WI
Division of Pulmonary and Critical Care Medicine, Medical College of Wisconsin, Milwaukee, WI,
Nina Friedly
Medical College of Wisconsin Department of Biomedical Engineering, Marquette University, Milwaukee, WI
Ranjan K. Dash
Medical College of Wisconsin Department of Biomedical Engineering, Marquette University, Milwaukee, WI
Andreas M. Beyer
Department of Medicine, Medical College of Wisconsin, Milwaukee, WI
Anne V. Clough
Department of Mathematics, Statistics, and Computer Science, Marquette University, Milwaukee, WI
Elizabeth R. Jacobs
Zablocki VA Medical Center, Milwaukee, WI
Division of Pulmonary and Critical Care Medicine, Medical College of Wisconsin, Milwaukee, WI

ABSTRACT

The objectives of this study were to develop a robust protocol to measure the rate of hydrogen peroxide (H_2O_2) production in isolated perfused rat lungs, as an index of oxidative stress, and to determine the cellular sources of the measured H_2O_2 using the extracellular probe Amplex red (AR). AR was added to the recirculating perfusate in an isolated perfused rat lung. AR's highly fluorescent oxidation product resorufin was measured in the perfusate. Experiments were carried out without and with rotenone (complex I inhibitor), thenoyltrifluoroacetone (complex II inhibitor), antimycin A (complex III inhibitor), potassium cyanide (complex IV inhibitor), or diohenylene iodonium (inhibitor of flavin-containing enzymes, e.g. NAD(P)H oxidase or NOX) added to the perfusate. We also evaluated the effect of acute changes in oxygen (O_2) concentration of ventilation gas on lung rate of H_2O_2 release into the perfusate. Baseline lung rate of H_2O_2 release was 8.45 ± 0.31 (SEM) nmol/min/g dry wt. Inhibiting mitochondrial complex II reduced this rate by 76%, and inhibiting flavin-containing enzymes reduced it by another 23%. Inhibiting complex I had a small (13%) effect on the rate, whereas inhibiting complex III had no effect. Inhibiting complex IV increased this rate by 310%. Increasing %O_2 in the ventilation gas mixture from 15 to 95% had a small (27%) effect on this rate, and this O_2-dependent increase was mostly nonmitochondrial. Results suggest complex II as a potentially important source and/or regulator of mitochondrial H_2O_2, and that most of acute hyperoxia-enhanced lung rate of H_2O_2 release is from nonmitochondrial rather than mitochondrial sources.

Introduction

There is ample evidence that oxidative stress plays a key role in the pathogenesis of acute and chronic lung diseases, with the pulmonary endothelium as a primary target [1–4]. Thus, the ability to assess oxidative stress and to determine the major cellular sources of oxygen radicals in intact functioning lungs is important to identify potential therapeutic targets for such conditions, and to assess the efficacy of novel therapies against oxidative stress [3].

Cellular sources of reactive oxygen species (ROS) can be classified as mitochondrial or nonmitochondrial [5]. More than 10 mitochondrial ROS generating sites have been identified, mostly in the electron transport chain (ETC) [6], which is widely accepted as a major source of ROS [1,4,6–11]. Complex I and complex III are reported to be the main sources of mitochondrial ROS under physiological and pathological conditions [5,9,10,12]. However, other studies have suggested complex II as another major source of ROS [13–16]. Nonmitochondrial ROS sources include NAD(P)H oxidase (NOX), xanthine oxidase, uncoupled endothelial nitric oxide synthase (eNOS), nitric oxide (NO) synthase, arachidonic acid metabolizing enzymes, peroxisomal fatty acid oxidation, and cytochrome P450s [5].

Previous studies have mostly used intracellular fluorescent probes, including 20, 70-dichlorodihydrofluorescein diacetate (DCF) for general ROS measurement [15,17,18] or hydroethidine (HE) for measuring superoxide production [19,20]. Following its reaction with ROS, DCF is oxidized to DCFH, which accumulates within cells since it is not cell-permeable, potentially interfering with cellular functions [17]. Similarly, HE binds to DNA after reacting with superoxide which could also interfere with cellular functions [17].

Unlike superoxide, hydrogen peroxide (H_2O_2) has a much longer half-life, is relatively stable, and can readily diffuse across the cellular membranes, and hence is a more robust index of oxidative stress over time [21,22]. Amplex red (AR) is a colourless and nonfluorescent extracellular probe, which is oxidized to coloured and highly fluorescent resorufin in the presence of H_2O_2 and horseradish peroxidase [22–24]. The objectives of this study were to develop a robust protocol to use AR to measure the rate of H_2O_2 production in isolated perfused rat lungs as an index of oxidative stress, to determine the cellular sources of the measured H_2O_2, and to assess the effect of high oxygen (O_2) tension in the lung ventilation gas mixture on the measured rate. The results suggest complex II as a potentially important source and/or regulator of mitochondrial H_2O_2 and a target for mitigating

oxidative stress, and that most of acute hyperoxia-enhanced lung rate of H_2O_2 release is from flavin-containing enzymes such as NAD(P)H oxidase rather than mitochondrial sources. To the best of our knowledge, this study is the first to evaluate the rate of H_2O_2 production in the isolated perfused rat lung and to determine the contributions of mitochondrial and nonmitochondrial sources of H_2O_2 to the measured rate.

Materials and methods

Materials

AR, horseradish peroxidase (HRP), and all other reagents used in experiments were purchased from Sigma Aldrich (St. Louis, MO, United States of America).

Isolated perfused rat lung preparation

Animal protocols described below were approved by the Institutional Animal Care and Use Committees of the Veterans Affairs Medical Center and Marquette University (Milwaukee, WI, United States of America). Adult male Sprague–Dawley rats (347 ± 4 g (SEM), n = 41) were used for this study. Each rat was anesthetized with sodium pentobarbital (40–50 mg/kg i.p.). The trachea was surgically isolated and cannulated, the chest opened and heparin (0.7 IU/g body wt.) injected into the right ventricle, as previously described [25]. The pulmonary artery and the pulmonary venous outflow were accessed via cannula, then the heart/lungs removed and connected to a ventilation-perfusion system. The Krebs–Ringer bicarbonate perfusate contained (in mM) 4.7 KCl, 2.51 $CaCl_2$, 1.19 MgSO4, 2.5 KH_2PO_4, 118 NaCl, 25 $NaHCO_3$, 5.5 glucose, and 3% bovine serum albumin [24–26]. The perfusion system was primed with the perfusate maintained at 37 C and equilibrated with 15% O_2, 6% CO_2, balance N_2 gas mixture resulting in perfusate PO_2, PCO_2 and pH of 105, 40 Torrs, and 7.4, respectively. The lung was ventilated (40 breaths/min) with the above gas mixture with endinspiratory and end-expiratory pressures of 6 and 3 mmHg, respectively. The pulmonary artery and airway pressures were referenced to atmospheric pressure at the level of the left atrium and monitored continuously during the course of the experiments. Perfusate was pumped (10 ml/min) through the lung until it was evenly blanched and venous effluent was clear of visible blood before switching from single pass to recirculation mode.

Experimental protocols

Lung baseline rate of H_2O_2 release and the effects of mitochondrial and flavin-containing enzymes inhibitors on this rate

The following experimental protocols were carried out in a dark room to minimize the photo-oxidation of AR. For all the experimental protocols, the total volume of the system was 25 ml, 5 of which were the perfusion system tubing and the lung vasculature (~0.8 ml) [27,28]. To start the experiment, the perfusate in the reservoir was emptied and replaced with 19 ml of perfusate with HRP (5 U/ml), AR (25 µM), and ascorbate oxidase (1 U/ml). Ascorbate oxidase was added to minimize the impact of ascorbate released by the lungs on the measured resorufin signal [29,30]. The flow (10 ml/min) was restarted (time 0 min) and 2ml reservoir samples were collected at times 1, 6, and 11 min. The sample collected at 1 min provided the background signal, whereas the samples at 6 and 11 min provided the baseline rate of lung H_2O_2 production as described in the data analysis section below. Immediately after each sample was collected from the reservoir, it was centrifuged for 1 min (13,000 g, 4 °C) to remove any cellular components and debris. The sample supernatant was then transferred into a plastic cuvette and its 610nm emission signal (545nm excitation) was measured using a RatioMaster fluorescence imaging system (Photon Technology International, HORIBA Scientific, NJ). The emission filter used is centred at 610nm (ET610/30M, Chroma, VT) with a bandwidth of 30 nm. After the signal was acquired, the sample was added back to the reservoir.

To determine the contribution of a given cellular source to the measured baseline rate, an inhibitor (see Table 1 for concentrations used and references for those concentrations) was added to the recirculating perfusate after the reservoir sample at 11 min was collected. This was followed by collecting reservoir samples at times 16, 21, and 26 min. Each sample was centrifuged in the same manner as described above and its emission signal was then measured, after which it was added back to the reservoir. Thus, for each lung the rate of H_2O_2 release was determined before and after the addition of one of the inhibitors in Table 1.

Table 1. Concentrations, solvents, volumes, and targets of inhibitors in the 25-ml recirculating perfusate of the ventilation-perfusion system.

Inhibitor	Target	Perfusate concentration	Vehicle	Stock volume added	Reference
ROT	Complex I	40 µM	DMSO	10 µl	[38,47]
TTFA	Complex II	20 µM	DMSO	12.5 µl	[38]
AA	Complex III	4 µM	95% Ethanol	5 µl	[48]
KCN	Complex IV	2 mM	0.2 mM KH_2PO_4	50 µl	[38,47,49]
DPI	Flavin-containing enzymes such as NAD(P)H oxidase (NOX)	5 µM	DMSO	7.9 µl	[50]

DMSO: Dimethyl sulfoxide; KH_2PO_4: 0.2-mM phosphate buffer; ROT: rotenone; TTFA: thenoyltrifluoroacetone; AA: antimycin A; KCN: potassium cyanide; DPI: diphenyleneiodonium chloride.

To determine the impact of the inhibitor vehicles (dimethyl sulfoxide (DMSO), KH_2PO_4, or 95% ethanol, see Table 1) alone on the lung rate of H_2O_2 release, the above protocol was repeated in a group of lungs with the vehicle only (instead of inhibitorþvehicle) added at time 11 min to the recirculating perfusate. For DMSO, the volume added to the 25 ml recirculation perfusate was 12.5 ml.

At the end of the above protocol, the lungs were removed from the system and their wet weight was measured. The lungs were then dried to normalize the measured rate of H_2O_2 release to dry lung weight as described in the data analysis section.

Lung-independent rate of AR conversion to resorufin (AR photo-oxidation rate)

AR can photo-oxidize to resorufin in the presence of HRP [31]. To estimate this photo-oxidation rate, AR and HRP were added to the reservoir of the ventilationperfusion system without the lungs connected to the system and with the flow rate set at 10 ml/min. The measured rate of resorufin formation without lungs in the circuit was attributed to AR photo-oxidation and was subtracted from the overall rate measured with the lungs connected to the ventilation-perfusion system as described in the data analysis section.

Effect of oxygen level in the ventilation gas on the lung rate of H_2O_2 release

To evaluate the effect of acute increases in FiO_2 on lung rate of H_2O_2 release, we measured the rate of H_2O_2 release following lung ventilation with either a normoxic gas mixture (15% O_2, 6% CO_2, balance N_2) or hyperoxic gas mixture (95% O_2þ5% CO_2). For each experiment, the lungs were initially ventilated with the normoxic gas mixture for the baseline H_2O_2 release rate. After collection of reservoir sample at 11 min of recirculation, the ventilation gas was switched to the hyperoxic gas mixture and the rate was measured again under hyperoxic conditions.

Subcellular sources of hyperoxia-enhanced

H_2O_2 production

To begin to determine the sources of the hyperoxiainduced increase in the lung rate of H_2O_2 release, in another group of lungs we measured the lungs baseline rate of H_2O_2 release and the rates in the presence of thenoyltrifluoroacetone (TTFA) with the lungs ventilated first with the normoxic gas mixture and then with the hyperoxic gas mixture.

Standard curves

For each experimental day, a standard curve was obtained as described below and used to convert resorufin signal to H_2O_2 concentration in the recirculation perfusate. Four tubes, each containing 4ml of perfusate that included HRP and AR at the same concentrations as those used in the lung experimental protocol described above were prepared. A predetermined volume of 0.2mM H_2O_2 was added to each of the four tubes for final H_2O_2 concentrations of 0, 1, 2, and 3 µM in tubes 1, 2, 3 and 4, respectively. For each tube, a 2 ml sample was then treated the same way as the samples collected from the reservoir with the lungs collected to the ventilation-perfusion system. Thus, each sample was centrifuged for 1 min (13,000 g, 4°C), after which its 610nm emission signal was measured. For a given inhibitor, the standard curve was repeated with the inhibitor added to the samples prior to the addition of H_2O_2 to determine if the inhibitor and/or its vehicle interfered with the resorufin signal. A standard curve experiment with catalase (150 U/ml) added to each sample prior to the addition of HRP, which catalyses the reduction of H_2O_2, was also carried out to demonstrate the specificity of the resorufin signal to H_2O_2.

Data analysis

Standard curve

For each standard H_2O_2 concentration, the resorufin fluorescent intensity was determined from the average of the intensity measurements acquired over a period of 5 sec. Sample values with no H_2O_2 added to the sample were considered background, and this intensity was subtracted from the intensities measured with different H_2O_2 concentrations added to the standard samples. The resulting intensities were then plotted against the known H_2O_2 concentrations added to each standard sample. Linear regression analysis was then used to estimate the slope of the standard curve which was used to convert resorufin intensity in a given reservoir sample (without or with lungs connected to the ventilation-perfusion system) to H_2O_2 concentration in the recirculating perfusate.

Analysis of reservoir samples without or with lungs connected to the ventilation-perfusion system

For each reservoir sample at a given sampling time, the measured intensity was determined as the average of the intensities acquired over a period of 5 sec. Sample values collected at time 1 min were considered background intensity and subtracted from the intensities of all subsequent samples. This time point is long enough for the perfusate in the reservoir and he rest of the ventilation-perfusion system to mix. The slope of the standard curve for each day of experiments was used to convert the measured intensity to H_2O_2 concentration in the recirculating perfusate at the time the reservoir sample was collected. The "equivalent" amount of H_2O_2 (in nmol) in the 25 ml recirculating perfusate was then obtained as the product of the H_2O_2 concentration and volume of recirculating perfusate (25 ml). The result of this analysis represents the amount of H_2O_2 in the system as a function of recirculation time with or without the lung attached to the ventilation-perfusion system. Using linear regression, the "equivalent" rates of H_2O_2 released without and with the lung attached to the perfusion system were then obtained. The difference was then used as the lung rate of H_2O_2 release (nmol/min).

To account for differences in lung weights, the measured rate of lung H_2O_2 release was normalized to lung dry weight and expressed as nmol/min/g dry lung wt.

The rate of "equivalent" H_2O_2 generation without the lungs attached to the perfusion system due to photo-oxidation was determined using a separate group of experiments ($n = 3$). The average rate of H_2O_2 generation (nmol/min) from three experiments without lungs in the circuit was subtracted from the rate of H_2O_2 generation with the lungs connected to the ventilation-perfusion system.

Statistical analysis

Statistical evaluation of data was carried out using SigmaPlot version 12.0 (Systat Software Inc, San Jose, CA). A paired t-test was used to compare lung rates of H_2O_2 measured before and after the addition of an inhibitor to the recirculating perfusate, or following lung ventilation with the normoxic or hyperoxic gas mixture. Values from different groups were compared using unpaired t-test or one-way ANOVA followed by followed by Tukey's range test to evaluate differences between means of groups. The level of statistical significance was set at $p < .05$. Values are mean ± SEM as indicated in the text unless otherwise indicated.

Results

Body weights, lung wet weights, lung wet/dry weight ratios, and pulmonary artery pressures

Table 2 shows that the rat body weights of the experimental groups were not different (ANOVA, $p = .311$). None of the experimental protocols had a significant effect (ANOVA) on lung wet weights ($p = .452$), wet/dry weight ratios ($p = .654$), or pulmonary artery pressures ($p = .385$).

BW, lung wet weights, wet/dry weight ratios, and pulmonary artery pressures.

Table 2. BW, lung wet weights, wet/dry weight ratios, and pulmonary artery pressures.

Treatment	BW (g)	Lung wet weight (g)	Wet/dry weight ratio	Artery Pressure (mmHg)
Ethanol (n = 3)	346 ± 9	1.23 ± 0.05	5.50 ± 0.16	6.3 ± 0.3
DMSO (n = 4)	339 ± 16	1.39 ± 0.06	5.65 ± 0.09	6.2 ± 0.2
KH_2PO_4 (n = 4)	350 ± 16	1.33 ± 0.05	5.60 ± 0.08	6.3 ± 0.3
ROT (n = 4)	379 ± 8	1.39 ± 0.03	5.49 ± 0.33	6.3 ± 0.4
95% O_2 (n = 4)	350 ± 9	1.26 ± 0.05	5.51 ± 0.14	6.6 ± 0.2
95% O_2+TTFA (n = 4)	326 ± 6	1.31 ± 0.07	6.17 ± 0.37	6.4 ± 0.3
TTFA (n = 6)	334 ± 11	1.28 ± 0.06	5.69 ± 0.31	6.3 ± 0.3
AA (n = 4)	341 ± 19	1.31 ± 0.06	5.92 ± 0.24	6.8 ± 0.3
KCN (n = 4)	350 ± 12	1.24 ± 0.03	5.51 ± 0.17	6.0 ± 0.2
DPI (n = 4)	363 ± 11	1.24 ± 0.04	5.59 ± 0.07	6.9 ± 0.3

Values are mean ± SEM, n is the number of lungs for a given treatment.
DMSO: dimethyl sulfoxide; KH_2PO_4: 0.2-mM phosphate buffer; ROT: rotenone; TTFA: thenoyltrifluoroacetone; AA: antimycin
A; KCN: potassium cyanide; DPI: diphenyleneiodonium chloride; BW: body weights.

Resorufin standard curve and the effects of inhibitors

Figure 1(A) shows a representative standard curve without and with catalase added to the standard samples to inhibit the oxidation of AR to resorufin. TTFA (Figure 1(B)), rotenone (data not shown), antimycin A (AA) (data not shown), and diphenyleneiodonium chloride (DPI) (data not shown) had no effect on the resorufin emission signal in the standard curve. Only potassium cyanide (KCN) had an effect on the resorufin emission signal (Figure

1(C)), appearing to quench the resorufin signal; the slope of the standard curve scaled down by ~60% as compared to that without KCN. This quenching effect was accounted for in the analysis of the resorufin signal measured in perfusate recirculating through the lungs in the presence of KCN.
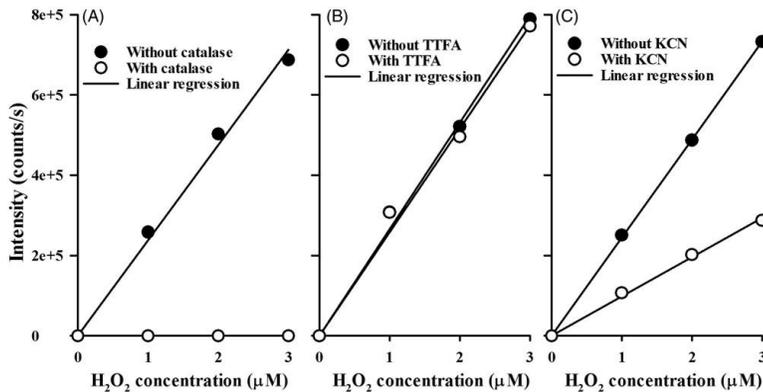

Figure 1. Panel A. Standard curves of AR oxidation to resorufin with (○) or without (•) catalase added to the standard curve samples. Panel B. Standard curves with (○) or without (•) thenoyltrifluoroacetone (TTFA) added to the standard curve samples. Panel C. Standard curves with (○) or without (•) potassium cyanide (KCN) added to the standard curve samples.

AR photo-oxidation rate

To determine the photo-oxidation rate of AR to resorufin in perfusate recirculating through the lungs, the slope of the standard curve exemplified in Figure 1(A) was used to convert the resorufin emission signal in reservoir samples collected without the lungs attached to the ventilation-perfusion system to "equivalent" nmol of H_2O_2 in the recirculating perfusate (Figure 2(A)). AR photo-oxidation rate to "equivalent" H_2O_2 formation was then estimated as the linear regression slope. This "equivalent" rate of H_2O_2 formation due to AR photo-oxidation to resorufin was 0.43 ± 0.02 (SEM, $n = 3$) nmol/min.
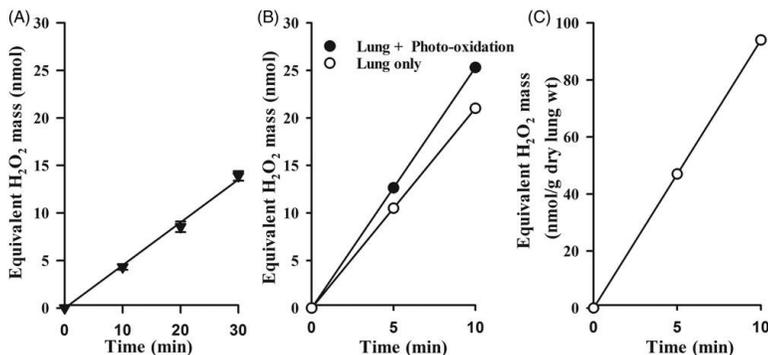

Figure 2. Panel A. Representative "equivalent" amount of H_2O_2 formed in the recirculating perfusate due to AR photo-oxidation to resorufin as a function of recirculation time following the addition of AR + HRP to the recirculating perfusate. Values are mean ± SEM (n = 3). Panel B. Representative "equivalent" amount of H_2O_2 in the recirculating perfusate as a function of recirculation time with the lungs connected to the ventilation-perfusion system before (•) and after (○) the mean rate of "equivalent" H_2O_2 formation due to AR photo-oxidation (Panel A) was subtracted. Panel C. Representative amount of H_2O_2 released from the lungs per gram of dry lung wt. as function of recirculation time.

To determine the lung rate of H_2O_2 release, the slope of the standard curve exemplified in Figure 1(A) was used to convert the resorufin emission signals in reservoir samples collected with the lungs attached to the ventilation-perfusion system to "equivalent" nmol of H_2O_2 in the recirculation perfusate as exemplified in Figure

2(B) (solid symbols). The slope of the resulting curve is interpreted as the sum of the rates of lung H_2O_2 release and AR photo-oxidation rate to resorufin. On average, AR photo-oxidation rate to resorufin (0.43 nmol/min) was ~18% of the total rate of resorufin formation with the lung connected to the ventilation perfusion system. The lung rate of H_2O_2 release (slope of the data exemplified in Figure 2(C)) is reported in units of nmol/min/g dry lung wt.

Lung rate of H_2O_2 release and the effects of mitochondrial and flavin-containing enzymes inhibitors on this rate

The lung rate of H_2O_2 release under normoxic ventilation conditions (15% O_2, 6% CO_2, balance N_2) was 8.45 ± 0.31 (SEM, $n = 41$) nmol/min/g dry lung wt. Figure 3 shows that lung treatment with the mitochondrial complex II inhibitor (TTFA) decreased the lung rate of H_2O_2 release by ~76% (paired t-test, $p = .002$), whereas lung treatment with the DPI (inhibitor of flavin-containing enzymes such as NOX) decreased the rate by ~23% (paired t-test, $p = .004$). Moreover, Figure 3 shows that lung treatment with the complex I inhibitor rotenone (ROT) had a small (~13%), but significant effect on the lung rate of H_2O_2 release (paired t-test, $p = .043$), whereas lung treatment with the complex III inhibitor AA had no significant effect on this rate (paired t-test, $p = .315$). On the other hand, lung treatment with complex IV inhibitor KCN increased the lung rate of H_2O_2 release by ~310% (paired t-test, $p = .004$). These results suggest that in normoxic lungs most of the rate of H_2O_2 release, and hence ROS formation, is from the mitochondrial electron transport chain. Baseline lung rates of H_2O_2 release for the different experimental conditions (Figure 3) are not significantly different (ANOVA, $p = .387$).
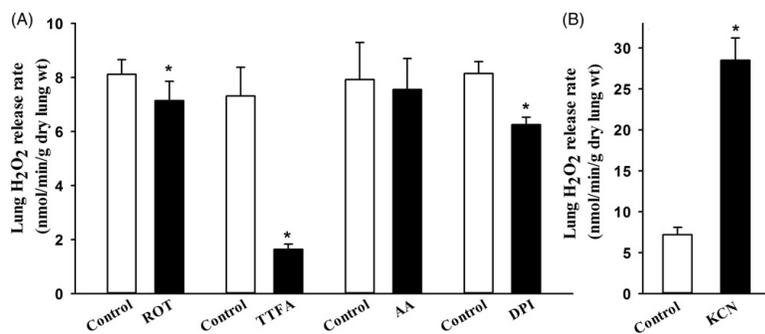

Figure 3. Panel A. Lung rates of H_2O_2 release before (control) and after the addition of rotenone (ROT, n = 4), thenoyltrifluoroacetone (TTFA, n = 6), AA (n = 4), or diphenyleneiodonium chloride (DPI, n = 4) to the recirculating perfusate. Panel B. Lung rates of H_2O_2 release before (control) and after the addition of potassium cyanide (KCN, n = 4) to the recirculating perfusate. Values are mean ± SEM. *significantly different from the corresponding rate without any inhibitor, paired t-test (p < 0.05).

Effects of vehicles of mitochondrial inhibitors and DPI on the measured lung rates of H_2O_2 release

Figure 4 shows that none of the vehicles had a significant effect (paired t-test, $p = .431.108$, and$.288$ for DMSO, phosphate buffer, and ethanol, respectively) on the measured lung rate on H_2O_2 release.
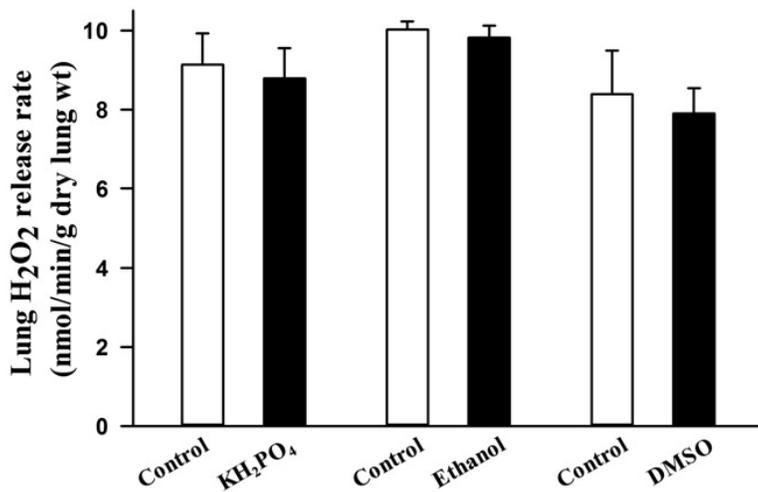
Figure 4. Lung rates of H_2O_2 release before (control) and after the addition of 50 µl 0.2-µM phosphate buffer (KH2PO4, n = 4), 5 µl 95% ethanol (n = 3), or 12.5 µl of dimethyl sulfoxide (DMSO, n = 4) to the 25-ml recirculating perfusate. Values are mean ± SEM.

Effect of % O_2 in ventilation gas mixture on the lung rate of H_2O_2 release

To evaluate the effect of acute changes in O_2 concentration in the ventilation gas mixture on lung rate of H_2O_2 release, we evaluated this rate following lung ventilation with either the normoxic gas mixture (15% O_2, 6% CO_2, balance N_2) or hyperoxic gas mixture (95% O_2 + 5% CO_2). Figure 5(A) shows that H_2O_2 release during ventilation with hyperoxic gas mixture (13.31 ± 0.58 nmol/min/g dry lung wt., $n = 4$) for 10 min was ~27% higher (paired t-test, $p = .026$) than that measured during ventilation with normoxic gas mixture.
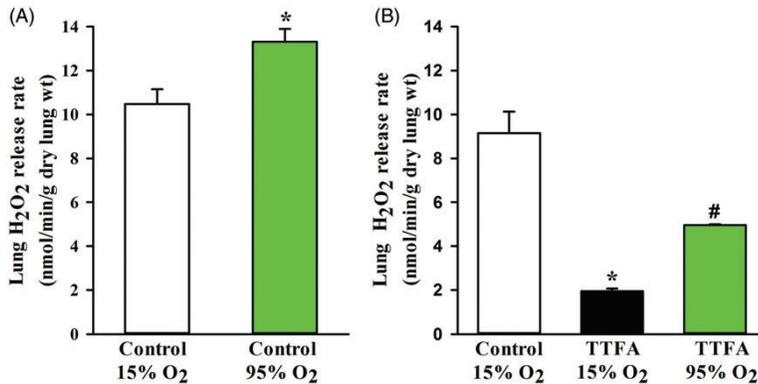

Figure 5. Panel A. Lung rates of H_2O_2 release during lung ventilation with normoxic (15% O_2) or hyperoxic (95% O_2) gas mixture (n = 4). Panel B. Baseline lung rates of H_2O_2 release (control) along with rates in the presence of thenoyltrifluoroacetone (TTFA) during lung ventilation with normoxic (15% O_2) or hyperoxic (95% O_2) gas mixture (n = 4). Values are mean ± SEM. *significantly different from control (15% O_2), #significantly different from TTFA (15% O_2), paired t-test (p < 0.05).

To begin to determine how much of this increase in the rate of lung H_2O_2 release at 95% O_2 is from mitochondrial sources and how much from flavin-containing enzymes, we measured the rate of H_2O_2 release in the presence of TTFA in lungs ventilated first with the normoxic gas mixture and then with the hyperoxic gas mixture. Figure 5(B) show that the rate of lung H_2O_2 release during ventilation with the hyperoxic gas mixture (4.96 ± 0.05 nmol/min/g dry lung wt., $n = 4$) was 154% larger than that during ventilation with the normoxic gas mixture (1.95 ± 0.11-nmol/min/g dry lung wt.). This increase is large enough to account for the hyperoxia-

induced increase in baseline lung rate of H_2O_2 release (Figure 5(A)), suggesting that most of the oxygen-dependent increase in lung H_2O_2 release is nonmitochondrial.

Discussion and conclusions

Our study describes a fluorometric approach for measuring the rate of H_2O_2 release from isolated perfused rat lungs, as an index of pulmonary oxidative stress, using the extracellular probe AR. For lungs from control rats ventilated with the normoxic gas mixture, the results show that inhibiting mitochondrial complex II reduced this rate by ~76%, and inhibiting flavin-containing enzymes reduced it by another ~23%. The results also show that inhibiting complex I had a small (~13%) effect on the rate, whereas inhibiting complex III had no effect on this rate. On the other hand, inhibiting complex IV increased the lung rate of H_2O_2 release by ~310%. Furthermore, increasing the oxygen concentration in the ventilation gas mixture from 15 to 95% had a relatively small (~27%), but significant effect on the lung rate of H_2O_2 release, and this acute oxygen-dependent increase was mostly nonmitochondrial. These results suggest that mitochondria are the main source of H_2O_2 released from lungs into the recirculating perfusate, that complex II is a potentially important source of H_2O_2 and a potential target for mitigating pulmonary oxidative stress, and that the hyperoxia-enhanced lung rate of H_2O_2 release acutely is most likely from flavin-containing enzymes such as NOX rather than mitochondrial sources.

AR has many advantages, including its minimal interaction with cellular functions, its sensitivity and specificity to H_2O_2, and its reduced background fluorescence in comparison to other fluorescent ROS probes [12,17,22,31,32]. Because AR is a measure of the H_2O_2 that has overwhelmed intracellular antioxidant defenses and leaked to the extracellular space, the rate of resorufin formation and hence the rate of H_2O_2 released into the extracellular space could be considered an index of oxidative stress experienced by the lung cells under a given condition. AR has been used previously to measure the rate of H_2O_2 production mostly in *in vitro* assays including isolated mitochondria, cultured cells, and tissue homogenates [12,31]. Few studies have used AR to measure the rate of H_2O_2 production in intact organs, including isolated perfused mouse lungs [19,24,26]. In those studies, the cellular sources of the measured H_2O_2 were not identified. In our investigations, changes in the measured lung rates of H_2O_2 release after inhibitors are reflective of changes in the rate of cellular ROS production. To the best of our knowledge, this is the first study measuring the rate of H_2O_2 release from isolated perfused rat lungs, identifying the main sources of this rate under physiological conditions, and evaluating the effect of acute hyperoxia on this rate.

Previously we reported the lung rate of O_2 consumption to be ~2.4-µmol/min/g dry lung wt. [38]. The baseline lung rate of H_2O_2 release measured in the present study under normoxic ventilation conditions is 8.45 ± 0.31 nmol/min/g dry lung wt. Since superoxide to O_2 stoichiometry is 1:1 and superoxide to H_2O_2 stoichiometry is 2:1, then the equivalent O_2 consumption rate of the measured lung rate of H_2O_2 release is ~17-nmol/min/g dry lung. This rate is ~0.7% of the rat lung rate of O_2 consumption, and hence within the 1-2% of the total O_2 consumption rate converted to ROS production, as suggested by A. Starkov [6]. In addition, it is consistent with results from a study by Makrecka-Kuka et al. in which they measured an H_2O_2 flux in permeabilised cells that was <1% of the O_2 flux [35].

Complex II is unique in that it couples the Krebs cycle and the ETC [14], although it does not contribute directly to the generation of the proton motive force. As such, the main function of complex II is to help keep the quinone pool reduced. An important and somewhat unexpected result is the large effect of inhibiting complex II on the lung rate of H_2O_2 release, and the relatively small effect of inhibiting complex I or complex III on this rate. The effect of TTFA, which inhibits complex II at the quinone reduction site [39], on the lung rate of H_2O_2 release could be due to complex II being an important source of ROS and/or via its effect on ROS production at complexes I and/or III [39]. Quinlan, et al. suggested that complex II may be a major source of ROS *in vivo* [14]. They showed that complex II can be a major source of ROS under conditions of low succinate concentration

(maximum rate at succinate concentration of ~400 μM, close to the physiological range) and inhibition of ubiquinone reoxidation via complex I and III (i.e. in the presence of complex I and III inhibitors rotenone and myxothiazol, respectively). Both ubisemiquinone and FAD semiquinone radicals can be electron sources for the generation of ROS at complex II, although evidence points to fully reduced FAD as the major source under such conditions [39]. These results suggest that the direct or indirect contribution of complex II to mitochondrial ROS production depends on substrate availability, mitochondrial membrane potential, and the activities of other ETC complexes [6,39].

Results from previous studies regarding the effect of inhibiting complex I on mitochondrial ROS production have not been consistent, with some showing an increase, while others showing a decrease or no change in rate of ROS production [10,17]. Brueckl, et al. measured capillary endothelial cells ROS production in isolated perfused rat lungs using the intracellular fluorescent probe DCF with the lungs ventilated with either a normoxic (21% O_2) or hyperoxic gas mixture (up to 70% O_2) [17]. The results show that DCF signal increased almost linearly with the O_2 concentration in the ventilation gas, which varied between 21 and 70%. In addition, they showed that lung treatment with rotenone reduced baseline DCF signal (and hence baseline ROS production) by ~60% and completely inhibited the hyperoxia-induced increase in DCF signal. These results are not consistent with the results from the present study. This could be in part due to differences in the two probes used (DCF vs. AR). Due to the extracellular nature of AR, it cannot be used for measuring the actual lung rate of H_2O_2 production from a specific source since the measured rate is the net of cellular H_2O_2 production at multiple sources and H_2O_2 scavenging rates. Another potential reason for differences could be that in the present study the measured rate of H_2O_2 is from the whole lung (all 40 different types of cells) instead of from just capillary endothelial cells in the study by Brueckl, et al. [17].

Brueckl, et al. also showed that DPI, an inhibitor of flavin-containing enzymes such as NOX, did not affect baseline DCF signal, but had a significant effect on hyperoxia-induced increase in DCF, especially towards the later phase of the 90 min exposure period [17]. They suggested that the early phase of hyperoxia-induced increase in DCF signal was due to an increase in mitochondrial ROS, but the later phase of the hyperoxia-enhanced DCF signal was due to activation of NOX by endothelial calcium signalling and Rac1 activation. DPI's lack of effect on baseline DCF signal is also not consistent with the effect of DPI on the lung rate of H_2O_2 release in the present study, although the contribution of NOX to hyperoxia-enhanced DCF signal is congruent with the results from the present study.

Ghanian, et al. measured the rate of superoxide production in the cultured fetal lamb pulmonary artery endothelial cells using the fluorescence probe MitoSOX Red, a derivative of hydroethidine [10]. They showed that inhibition of complex I with rotenone increased superoxide production as measured by MitoSOX Red signal by ~60%. Additional results show that treatment of cells with AA or potassium cyanide (KCN) also increased superoxide production by ~130 and 60%, respectively. The results with rotenone and AA are inconsistent with the results of the present study or the study by Brueckl, et al. [17] with respect to the effect of rotenone on ROS production. Differences between cultured cells and organs and/or probes used could account for this apparent inconsistency. The increase in superoxide production in the presence of KCN reported by Ghanian, et al. is consistent with the results in the present study, although the increase is smaller than the measured KCN-induced increase in the lung rate of H_2O_2 release in the present study [10]. Ghanian, et al. concluded that complexes I, III and IV are major sources of superoxide in cultured pulmonary endothelial cells [10]. The effect of KCN on the lung rate of H_2O_2 release in the present study could be indicative of complex IV being a source of ROS, especially since in the present study inhibiting complex III with AA had no significant effect on the lung rate of H_2O_2 release.

Previous studies have reported an increase in ROS production with the addition of AA in reduced systems (e.g. cells and submitochondrial particles) [12,40]. Those results are not consistent with the results from the present

study. Again, this could be to differences between reduced systems and intact functioning lung and/or differences between the probes and/or substrates.

Using AR, Lee, et al. measured the rate of H_2O_2 release by isolated perfused lungs from normal mice and from mice 24 hours after treatment with lipopolysaccharin (LPS) to induce lung injury [24,26]. They showed that LPS increased lung rate of H_2O_2 release by more than 9-fold and that ~90% of this increase was due to the NOX isomer NOX2. However, NOX2 does not appear to contribute much to the baseline rate of lung H_2O_2 release. Our data show that ~75% of the basal lung rate of H_2O_2 release is from the mitochondria, and ~23% from flavin-containing enzymes, potentially NOX2 and/or NOX4. For the above studies by Lee, et al., the baseline rate of mouse lung H_2O_2 release was 0.011-nmol/min/g dry lung wt., which is very small compared to the rate in rat lungs (8.45 nmol/min/g dry lung wt.) in the present study. This could be due to species differences and/or differences in the approach used to convert resorufin signal to H_2O_2. Lee et al. [24,26] used Amplex red's extinction coefficient (54000 cm^{-1} M^{-1}) for the conversion, whereas in the present study a standard curve with known H_2O_2 concentrations was used.

Previous studies have suggested that the lung rate of ROS formation is dependent on the level of O_2 in the ventilation gas mixture [17,41]. Results of the present study show that increasing the O_2 concentration in the ventilation gas mixture from 15 to 95% O_2 had only a small (27%) effect on the lung rate of H_2O_2 release, and suggest that this O_2-dependent increase was mostly nonmitochondrial (Figure 5). The results of the present study with acute hyperoxia may not be reflective of the sources of pulmonary oxidative stress in chronic hyperoxia, which others and we have used as a model of human acute respiratory distress syndrome (ARDS) [25].

At least three of the known NOX isomers, NOX2, NOX3, and NOX4, are present in lung tissue [2]. The results of the present study are consistent with NOX4 being the main NOX source of the lungs rate of H_2O_2 release since its rate of ROS formation has a relatively large Michaelis-Menten constant (K_m = ~18%) for O_2 [41] as compared to that for NOX2 (K_m = ~2-3%). NOX4, which is present in the pulmonary artery endothelial and smooth muscle cells, and in the myofibroblasts in the airways is unique since it produces ROS mainly (90%) as H_2O_2 rather than superoxide from molecular O_2, and is regulated by O_2 level [41]. In addition, because of its relatively high K_m for O_2, NOX4 may serve as an O_2 sensor in cells, with H_2O_2 as the signalling molecule [41].

Limitations of AR in the isolated perfused rat lung

AR provides a robust approach for measuring the rate of H_2O_2 release from isolated perfused lungs. However, due to its extracellular nature AR cannot be used to measure the actual lung rate of H_2O_2 production or the rate of production from a specific source since the measured rate is the net of the rates of cellular H_2O_2 production and H_2O_2 scavenging. In addition, a given inhibitor can affect H_2O_2 production at multiple sources as discussed above.

The lung consists of 40 different cell types [45,46]. The results using AR provide no direct information regarding the contributions of the different cell types to the measured lung rate of H_2O_2 release, although endothelial cells would be expected to dominate because of their large surface area and high fraction (~50%) of total lung cells, and their direct contact with AR in perfusate [44]. Although the question regarding the contributions of specific cell types will be important for future studies, alteration in the lung rate of H_2O_2 release as an index of pulmonary oxidative stress has functional implications regardless of the lung cell types involved.

To the best of our knowledge, this study is the first to evaluate the rate of H_2O_2 production in the isolated perfused rat lung and to determine the contributions of mitochondrial and nonmitochondrial sources of H_2O_2 to the measured rate. This approach could be used to assess the role of oxidative stress in the pathogenesis of

acute and chronic lung diseases and the efficacy of novel therapies for mitigating oxidative stress in intact functioning lungs.

Acknowledgments

Disclosure statement

No potential conflict of interest was reported by the authors.

References

[1] Mittal M, Siddiqui MR, Tran K, et al. Reactive oxygen species in inflammation and tissue injury. Antioxid Redox Signal. 2014;20(7):1126–1167.

[2] Griffith B, Pendyala S, Hecker L, et al. NOX enzymes and pulmonary disease. Antioxid Redox Signal. 2009; 11(10):2505–2516.

[3] Audi SH, Jacobs ER, Zhang X, et al. Protection by inhaled hydrogen therapy in a rat model of acute lung injury can be tracked in vivo using molecular imaging. Shock. 2017;48(4):467–476.

[4] Andreyev AY, Kushnareva YE, Starkov AA. Mitochondrial metabolism of reactive oxygen species. Biochemistry (Mosc). 2005;70(2):200–214.

[5] Zhang DX, Gutterman DD. Mitochondrial reactive oxygen species-mediated signaling in endothelial cells. Am J Physiol Heart Circ Physiol. 2007;292(5): H2023–H2031.

[6] Starkov AA. The role of mitochondria in reactive oxygen species metabolism and signaling. Ann N Y Acad Sci. 2008;1147:37–52.

[7] Cloonan SM, Choi AM. Mitochondria: commanders of innate immunity and disease? Curr Opin Immunol. 2012;24(1):32–40.

[8] West AP, Shadel GS, Ghosh S. Mitochondria in innate immune responses. Nat Rev Immunol. 2011;11(6): 389–402.

[9] Turrens JF. Mitochondrial formation of reactive oxygen species. J Physiol. 2003;552(2):335–344.

[10] Ghanian Z, Konduri GG, Audi SH, et al. Quantitative optical measurement of mitochondrial superoxide dynamics in pulmonary artery endothelial cells. J Innov Opt Heal Sci. 2018;11(1):1750018-1–1750018-16.

[11] Murphy MP. How mitochondria produce reactive oxygen species. Biochem J. 2009;417(1):1–13.

[12] Chen Q, Vazquez EJ, Moghaddas S, et al. Production of reactive oxygen species by mitochondria: central role of complex III. J Biol Chem. 2003;278(38): 36027–36031.

[13] Hoekstra AS, Bayley JP. The role of complex II in disease. Biochim Biophys Acta. 2013;1827(5):543–551.

[14] Quinlan CL, Orr AL, Perevoshchikova IV, et al. Mitochondrial complex II can generate reactive oxygen species at high rates in both the forward and reverse reactions. J Biol Chem. 2012;287(32): 27255–27264.

[15] Paddenberg R, Ishaq B, Goldenberg A, et al. Essential role of complex II of the respiratory chain in hypoxiainduced ROS generation in the pulmonary vasculature. Am J Physiol Lung Cell Mol Physiol. 2003;284(5): L710–L719.

[16] Valls-Lacalle L, Barba I, Mir_o-Casas E, et al. Succinate dehydrogenase inhibition with malonate during reperfusion reduces infarct size by preventing mitochondrial permeability transition. Cardiovasc Res. 2016; 109(3):374–384.

[17] Brueckl C, Kaestle S, Kerem A, et al. Hyperoxia-induced reactive oxygen species Formation in Pulmonary Capillary Endothelial Cells in situ. Am J Respir Cell Mol Biol. 2006;34(4):453–463.

[18] Kalyanaraman B, Darley-Usmar V, Davies KJ, et al. Measuring reactive oxygen and nitrogen species with fluorescent probes: challenges and limitations. Free Radic Biol Med. 2012;52(1):1–6.

[19] Chatterjee S, Chapman KE, Fisher AB. Lung ischemia: a model for endothelial mechanotransduction. Cell Biochem Biophys. 2008;52(3):125–138.

[20] Li N, Ragheb K, Lawler G, et al. Mitochondrial complex I inhibitor rotenone induces apoptosis through enhancing mitochondrial reactive oxygen species production. J Biol Chem. 2003;278(10):8516–8525.

[21] Bienert GP, Schjoerring JK, Jahn TP. Membrane transport of hydrogen peroxide. Biochim Biophys Acta. 2006;1758(8):994–1003.

[22] Dikalov SI, Harrison DG. Methods for detection of mitochondrial and cellular reactive oxygen species. Antioxid Redox Signal. 2014;20(2):372–382.

[23] Rhee SG, Chang TS, Jeong W, et al. Methods for detection and measurement of hydrogen peroxide inside and outside of cells. Mol Cells. 2010;29(6): 539–549.

[24] Lee I, Dodia C, Chatterjee S, et al. Protection against LPS-induced acute lung injury by a mechanism-based inhibitor of NADPH oxidase (type 2). Am J Physiol Lung Cell Mol Physiol. 2014;306(7):L635–L644.

[25] Audi SH, Clough AV, Haworth ST, et al. 99MTc- Hexamethylpropyleneamine oxime imaging for early detection of acute lung injury in rats exposed to hyperoxia or lipopolysaccharide treatment. Shock. 2016;46(4):420–430.

[26] Lee I, Dodia C, Chatterjee S, et al. A novel nontoxic inhibitor of the activation of NADPH oxidase reduces reactive oxygen species production in mouse lung. J Pharmacol Exp Ther. 2013;345(2):284–296.

[27] Audi SH, Bongard RD, Krenz GS, et al. Effect of chronic hyperoxic exposure on duroquinone reduction in adult rat lungs. Am J Physiol Lung Cell Mol Physiol. 2005;289(5):L788–L797.

[28] Ramakrishna M, Gan Z, Clough AV, et al. Distribution of capillary transit times in isolated lungs of oxygentolerant rats. Ann Biomed Eng. 2010;38(11):3449–3465.

[29] Audi SH, Bongard RD, Okamoto Y, et al. Pulmonary reduction of an intravascular redox polymer. Am J Physiol Lung Cell Mol Physiol. 2001;280(6): L1290–L1299.

[30] Rodrigues JV, Gomes CM. Enhanced superoxide and hydrogen peroxide detection in biological assays. Free Radic Biol Med. 2010;49(1):61–66.

[31] Zhao B, Summers FA, Mason RP. Photooxidation of Amplex Red to resorufin: implications of exposing the Amplex Red assay to light. Free Radic Biol Med. 2012; 53(5):1080–1087.

[32] Zhou M, Diwu Z, Panchuk-Voloshina N, et al. A stable nonfluorescent derivative of resorufin for the fluorometric determination of trace hydrogen peroxide: applications in detecting the activity of phagocyte NADPH oxidase and other oxidases. Anal Biochem. 1997;253(2):162–168.

[33] Messier EM, Bahmed K, Tuder RM, et al. Trolox contributes to Nrf2-mediated protection of human and murine primary alveolar type II cells from injury by cigarette smoke. Cell Death Dis. 2013;4:e573.

[34] Chen LJ, Li WD, Li SF, et al. Bleomycin induces upregulation of lysyl oxidase in cultured human fetal lung fibroblasts. Acta Pharmacol Sin. 2010;31(5):554–559.

[35] Makrecka-Kuka M, Krumschnabel G, Gnaiger E. Highresolution respirometry for simultaneous measurement of oxygen and hydrogen peroxide fluxes in permeabilized cells, tissue homogenate and isolated mitochondria. Biomolecules. 2015;5(3):1319–1338.

[36] Triantafyllou A, Bikineyeva A, Dikalova A, et al. Antiinflammatory activity of Chios mastic gum is associated with inhibition of TNF-alpha induced oxidative stress. Nutr J. 2011;10:64.

[37] Mishin V, Gray JP, Heck DE, et al. Application of the Amplex red/horseradish peroxidase assay to measure hydrogen peroxide generation by recombinant microsomal enzymes. Free Radic Biol Med. 2010;48(11): 1485–1491.

[38] Audi SH, Bongard RD, Dawson CA, et al. Duroquinone reduction during passage through the pulmonary circulation. Am J Physiol Lung Cell Mol Physiol. 2003; 285(5):L1116–L1131.

[39] Dr€ose S. Differential effects of complex II on mitochondrial ROS production and their relation to cardioprotective pre- and postconditioning. Biochim Biophys Acta. 2013;1827(5):578–587.

[40] Park WH, Han YW, Kim SH, et al. An Ros generator, antimycin A, inhibits the growth of HeLa cells via apoptosis. J Cell Biochem. 2007;102(1):98–109.

[41] Nisimoto Y, Diebold BA, Cosentino-Gomes D, et al. Nox4: a hydrogen peroxide-generating oxygen sensor. Biochemistry. 2014;53(31):5111–5120.

[42] Kallet RH, Matthay MA. Hyperoxic acute lung injury. Respir Care. 2013;58(1):123–141.

[43] Reiss LK, Uhlig U, Uhlig S. Models and mechanisms of acute lung injury caused by direct insults. Eur J Cell Biol. 2012;91(6–7):590–601.

[44] Crapo JD, Barry BE, Foscue HA, et al. Structural and biochemical changes in rat lungs occurring during exposures to lethal and adaptive doses of oxygen. Am Rev Respir Dis. 1980;122(1):123–143.

[45] Kotton DN, Morrisey EE. Lung regeneration: mechanisms, applications and emerging stem cell populations. Nat Med. 2014;20(8):822–832.

[46] Dinh PC, Cores J, Hensley MT, et al. Derivation of therapeutic lung spheroid cells from minimally invasive transbronchial pulmonary biopsies. Respir Res. 2017;18(1):132.

[47] Staniszewski K, Audi SH, Sepehr R, et al. Surface fluorescence studies of tissue mitochondrial redox state in isolated perfused rat lungs. Ann Biomed Eng. 2013; 41(4):827–836.

[48] Bongard RD, Yan K, Hoffmann RG, et al. Depleted energy charge and increased pulmonary endothelial permeability induced by mitochondrial complex I inhibition are mitigated by coenzyme Q1 in the isolated perfused rat lung. Free Radic Biol Med. 2013;65: 1455–1463.

[49] Sepehr R, Audi SH, Staniszewski KS, et al. Novel flurometric tool to assess mitochondrial redox state of isolated perfused rat lungs after exposure to hyperoxia. IEEE J Transl Eng Health Med 2013;1:1500210-1–1500210-10.

[50] Dodd-O JM, Pearse DB. Effect of the NADPH oxidase inhibitor apocynin on ischemia-reperfusion lung injury. Am J Physiol Heart Circ Physiol 2000;279(1): H303–H312.